Chinese Chemical Letters 35 (2024) 108324

Contents lists available at ScienceDirect

Chinese Chemical Letters

journal homepage: www.elsevier.com/locate/cclet

Synergic catalysis of W and Ni originating from substitution of trivacant phosphotungstate for the selective oxidation of aniline to azoxybenzene

Sheng Cai[a,b], Xiao-Yuan Wu[a], Weiming Wu[a], Sa-Sa Wang[a,*], Can-Zhong Lu[a,b,c,d,*]

[a] CAS Key Laboratory of Design and Assembly of Functional Nanostructures, and Fujian Provincial Key Laboratory of Nanomaterials, Fujian Institute of Research on the Structure of Matter, Chinese Academy of Sciences, Fuzhou 350002, China
[b] College of Chemistry and Materials Science, Fujian Normal University, Fuzhou 350117, China
[c] Xiamen Institute of Rare Earth Materials, Chinese Academy of Sciences, Xiamen 361021, China
[d] University of Chinese Academy of Sciences, Beijing 100049, China

ARTICLE INFO

Article history:
Received 10 January 2023
Revised 23 February 2023
Accepted 8 March 2023
Available online 15 March 2023

Keywords:
Polyoxometalate
{Ni_6} cluster
Modulated catalytic property
Aniline oxidation
Azoxybenzene

ABSTRACT

Partial substitution of polyoxometalate (POM) is an efficient route to modulate the catalytic property of maternal POM. In this work, a new Keggin type POM involving {Ni_6} cluster, {[$Ni(H_2O)_2(Dach)_2$][$Ni(Dach)_2$]$_2$}{[$Ni_6Cl(\mu$-OH)$_3(H_2O)(Dach)_3(WO_4)(PW_9O_{34})$][$Ni_6(\mu$-OH)$_3(H_2O)_2(Dach)_3(WO_4)(PW_9O_{34})$]}Cl·$27H_2O$, (**1**, Dach = 1,2-diaminocyclohexane) was synthesized. Compounds **1** shows excellent catalytic performance in the selective oxidation of aniline to azoxybenzene (AOB) in water. The apparently different results from that with the matrix {PW_9O_{34}} ({PW_9}) suggest the successful regulation of the catalytic property of {PW_9} by the introduction of the {Ni_6} cluster into the skeleton. The experimental results indicate that the highlighted performance of **1** is contributed by the synergy of W and Ni sites, which are respectively responsible for the oxidation and condensation steps in the production of AOB. The good selectivity to AOB is essentially attributed to the effective modulation of the reaction rates of oxidation and condensation steps by W and Ni sites, respectively.

Polyoxometalates (POMs) exhibit considerable potential for catalysis thanks to their outstanding redox properties [1,2]. In order to further improve the catalytic performances and expand the applications of POMs, many strategies have been used to create new POM-based materials including covalent inorganic-organic hybridization [3–6], introduction of secondary (multiple) metal(s) into the skeleton [7–11], encapsulating them into the channels of porous materials [12–15], employing them as the nodes of metal-organic frameworks (MOFs) [16–19], supporting them on functional materials [20,21], and assembling them into micelles or other structures [22–24], *etc*. Among them, bi-metallic POMs resulting from substitution of POMs receive most extensive attention for following reasons: (1) The introduction of secondary metal into POM skeleton modulates the electronic behavior of the POM matrix, consequently changes its catalytic property to meet the requirements of different reactions; (2) The introduced secondary metal may act as catalytically active site to endow the entirety with new catalytic property; (3) The introduced metal can act as new coordination site to construct extended POM-based framework, resultantly further improve the catalytic property of POM. So far, innumerable bi-metallic POM catalysts for various reactions have been created [1,2,25-27]. However, the demonstration of bi-functionality respectively deriving from two metals has less been reported.

Ni substituted POMs have shown excellent catalytic properties in the evolution of hydrogen/oxygen [14,28-30]. However, the catalytic properties of them for organic reactions, especially for oxidative reactions, remain largely unexplored. The lagging progress may be caused by the dramatically weakened redox capacity of the POM matrix caused by the introduction of Ni element, which is usually used for reductive reactions [31]. But the very feature of Ni substituted POMs is profitable for complicated multi-step oxidative reactions that produce multiple products such as the oxidation of aniline, which has been regarded as carcinogen to human beings. The oxidation of aniline produces several high value-added chemicals such as nitrosobenzene (NSB), nitrobenzene (NB), azobenzene (AB), and AOB (Scheme 1). However, these products are usually yielded concomitantly, resulting in poor selectivity to each product, because the initial product NSB is highly active, and

* Corresponding authors.
E-mail addresses: wss@fjirsm.ac.cn (S.-S. Wang), czlu@fjirsm.ac.cn (C.-Z. Lu).

https://doi.org/10.1016/j.cclet.2023.108324
1001-8417/

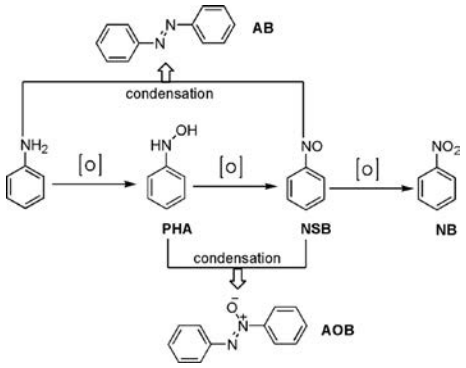

Scheme 1. The oxidation of aniline.

consequently prefers to undergo further oxidation to NB and condensation with aniline/intermediate phenylhydroxylamine (PHA) to AB/AOB. Recently, Wei's group achieved AB/AOB with high selectivity by changing additive and solvent in the presence of a POM catalyst $[N(C_4H_9)_4]_2[Mo_6O_{19}]$ [32]; Niu *et al.* respectively realized thermal/photo-catalytic transformation of aniline to AB/AOB in the presence of Ru-containing POMs [33,34]; Ma's group obtained high selectivity to NB/AB/AOB by changing oxidants and solvents with $Zr(OH)_4$ as the catalyst [35]. However, as one of the most important parameters in catalytic system, the work on the modulation of catalyst property is less reported.

In this work, a POM aggregate $\{[Ni(H_2O)_2(Dach)_2][Ni(Dach)_2]_2\}\{[Ni_6Cl(\mu\text{-}OH)_3(H_2O)(Dach)_3(WO_4)(PW_9O_{34})][Ni_6(\mu\text{-}OH)_3(H_2O)_2(Dach)_3(WO_4)(PW_9O_{34})]\}Cl\cdot 27H_2O$ (**1**) based on Keggin type $\{Ni_6\}$-capped phosphotungstate ($\{Ni_6PW_9\}$) subunit were synthesized by the reaction of $Na_9PW_9O_{34}\cdot nH_2O$ with $NiCl_2\cdot 6H_2O$ in the presence of auxiliary ligand Dach. Aggregate **1** is achieved by small $\{WO_4\}$ linkers that *in-situ* form through the decomposition of the starting material under reaction condition. To the best of our knowledge, aggregate **1** is the first 1D POM framework based on $\{Ni_6XW_9\}$ (X = P, Si) building blocks and tetrahedral $\{WO_4\}$ linkers. The catalytic performance of **1** in the selective oxidation of aniline in water, one of the most desirable solvent, was investigated. Compound **1** preferably produces AOB, while $\{PW_9\}$ shows a noncommittal selectivity to each product, suggesting the success of regulating the catalytic property of matrix $\{PW_9\}$ by the introduction of $\{Ni_6\}$ cluster. The highlighted performance of **1** in the production of AOB is attributed to the synergy of W and Ni sites. They are respectively responsible for the oxidation and condensation steps in the production of AOB from aniline. Essentially, the combination of $\{PW_9\}$ and $\{Ni_6\}$ cluster effectively modulates the rate of each reaction step, leading to excellent conversion of aniline (99.4%) and high selectivity to AOB (86.0%).

Crystallographic data of **1** reveal that it crystallizes in triclinic space group *P*-1 and presents one-dimensional structure containing two kinds of POM blocks 1A and 1B, which share identical skeleton that can be described as trilacunary Keggin type {B-α-PW_9O_{34}} units capped by $\{Ni_6\}$ clusters except one coordinating water ligand in 1A is replaced by Cl^- in 1B (Fig. 1). The bond length of Ni−Cl in 1B is 2.352(4) Å, much longer than that of Ni−O_w bond (2.074(7) Å) at the same site in 1A. Six Ni^{2+} ions in the $\{Ni_6\}$ cluster are arranged in a triangular plane and linked together by three μ_3-OH groups and seven μ_3-O/μ_4-O atoms from the matrix $\{PW_9\}$. Besides, the $\{Ni_6\}$ cluster is coordinated by three Dach ligands at the periphery. Blocks 1A and 1B are arranged alternately in the zigzag chain of **1**. They are linked together by *in-situ* produced $\{WO_4\}$ groups *via* the coordination of $\{Ni_6\}$ cluster with the bridge $\{WO_4\}$. The distances between W and O atoms in the tetrahedral $\{WO_4\}$ groups vary from 1.755(7) Å to 1.788(7) Å

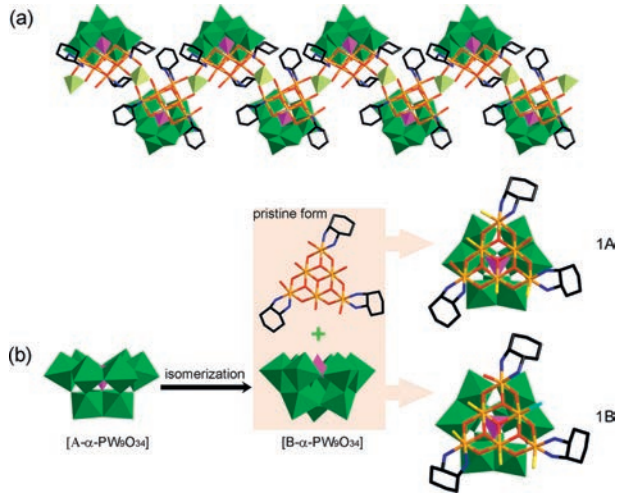

Fig. 1. (a) Crystallographic structure of **1**. (b) The formation process of the structural motifs 1A and 1B (Polyhedron: green W, yellowish green W, purple P; atom: red O, yellow replacing O, blue N, black C, orange Ni, greenish blue Cl).

and the O−W−O angles lie in the range of 106.6(4)°−111.6(4)°, well matching to those for $Na_2WO_4\cdot 2H_2O$ (W−O bond length: 1.759(7)−1.805(7) Å; O−W−O angles: 107.1(3)° − 112.4(3)°). The values are indicative of the maintaining of the geometrical configuration of $\{WO_4\}$. No apparent configuration distortion happens after coordinating with the $\{Ni_6\}$ cluster. Furthermore, the lengths of Ni−O bonds formed by the coordination of the bridging $\{WO_4\}$ and the $\{Ni_6\}$ cluster are in the range of 2.025(7)−2.143(7) Å, in line with that of normal Ni−O bond. These values confirm that $\{WO_4\}$ group is an ideal bridge for the construction of $\{Ni_6XW_9\}$-based framework, and consequently the formation of **1** is not accidental. The configuration of trilacunary $\{PW_9\}$ in 1A and 1B is B-α type, suggesting the configuration transformation from A-α to B-α under reaction temperature (Fig. 1b). The isomerization provides benign opportunity for the formation of the planar triangular $\{Ni_6\}$ cluster at the lacunary site. The *in-situ* formation of the tetrahedral $\{WO_4\}$ bridges is regarded to happen during the isomerization process.

It has been observed that the production of **1** is accompanied by trace hexagonal prism crystals of $[Ni_6(\mu\text{-}OH)_3(H_2O)_6(Dach)_3PW_9O_{34}]\cdot 7H_2O$ (**2**) (Fig. S1 in Supporting information). Crystallographic data reveal that **2** is a discrete POM that shares similar skeleton to 1A and 1B and packs into interesting wheel that seems to the previously reported POM aggregates $\{Ni_{36}(SiW_9)_6\}$ [36] and $\{Ni_{30}(PW_9)_6\}$ [37]. The cyclohexyl of Dach may play an important role in the packing process. The triangular $\{Ni_6\}$ cluster in **2** holds six water ligands at the edges in the manner of 2 + 2 + 2. In order to promote the yield of **2**, we have attempted to modulate the pH value of the reaction system, which probably impact on the isomerization process. The plan was carried out by changing the amount of Dach, rather than extra additives. When the amount of Dach decreased to 1.17 mmol from 5 mmol, the yield of **2** was enhanced, and **1** was absent in the reaction. Pure crystals of **2** were expediently collected by filtration after removing light pulverous impurities.

Based on the successful isolation of **2**, the pristine form of the $\{Ni_6\}$ cluster in **1** is also supposed to hold six coordinating water molecules that take the distribution manner of 1 + 2 + 3, quite different from that in **2**. Four of them are replaced by oxygen atoms of the tetrahedral $\{WO_4\}$ linkers. The alone water ligand in block 1B is replaced by Cl^-. The zigzag chains of **1** are negatively charged. The charges are balanced by positive $[Ni(H_2O)_2(Dach)_2]^{2+}$ and $[Ni(Dach)_2]^{2+}$ complexes that closely surround the chains to regularly arrange them in ABAB mode (Fig. S2 in Supporting in-

formation). Besides, abundant hydrogen bonds between the positively charged complexes and the POM chains are also observed (Table S1 in Supporting information). The strong electrostatic interactions and relatively weak hydrogen bonds make the structure pack tightly.

The phase purities of **1** and **2** are confirmed by PXRD analysis (Fig. S3 in Supporting information). The FT-IR spectra of them are presented in Fig. S4 (Supporting information). Two compounds show identical strong absorptions in the range of 1042−700 cm^{-1}. The peaks at 1042 and 940 cm^{-1} are engendered by the stretching vibrations of P−O and W−O_t, respectively. Those at 845, 794, 714 cm^{-1} are ascribed to the stretching vibration of W−O_b−W and that at 410 cm^{-1} is caused by the stretching vibration of Ni−O. The TGA curves of **1** and **2** are shown in Fig. S5 (Supporting information). The weight loss of 6.8% before 200 °C for **1** corresponds to the removal of twenty-seven lattice water molecules and five coordinating water molecules, and that of 7.2% before 280 °C for **2** corresponds to the removal of seven lattice water molecules and six coordinating water molecules. The burning of organic moieties occurs at 320 °C and 370 °C for **1** and **2**, respectively. The elemental composition and the oxidation states of constituent elements of **1** and **2** are identified by XPS (Figs. S6 and S7 in Supporting information). The full spectra reveal the presence of C, N, O, P, Cl, Ni and W elements in **1**, and the presence of C, N, O, P, Ni and W elements in **2**. The high resolution spectra of C, N, P, Ni and W for **1** and **2** are very similar. Taking compound **1** for example, two peaks of C 1s at 285.3 and 284.5 eV represent the C−N and C−C environments of Dach, respectively. Meanwhile, the peak of N 1s is centered at 399.76 eV, implying the sole environment of N. The spectrum of P 2p is fitted with two peaks centered at 134.34 and 133.49 eV that are respectively ascribed to P $2p_{1/2}$ and P $2p_{3/2}$ with 0.85 eV binding energy difference. The peaks of Ni 2p centered at 872.9 and 855.5 eV are assigned to the bivalent state Ni^{2+} $2p_{1/2}$ and Ni^{2+} $2p_{3/2}$, with two satellite peaks locating at 880.1 and 861.9 eV, respectively. The spectrum of W 4f exhibits two peaks at 37.5 eV ($4f_{5/2}$) and 35.4 eV ($4f_{7/2}$), suggesting the oxidation state of W in **1** is +6. Besides, the Cl 2p signal of **1** exhibits two peaks at 199.1 eV and 197.6 eV that are assigned to Cl $2p_{1/2}$ and Cl $2p_{3/2}$. Variable-temperature magnetic susceptibilities of **1** and **2** were also measured in the temperature range of 2–300 K with an external magnetic field of 1 kOe (Fig. S8 in Supporting information). The results reveal that **1** and **2** are dominantly ferromagnetic.

The catalytic performance of **1** was evaluated in water with 30% H_2O_2 as the oxygen source and without any additives. Initially, the reaction temperatures were screened in the range of room temperature to 70 °C. Only 40.2% aniline is converted at room temperature (*ca.* 17 °C) with the ratio of $n_{H_2O_2}:n_{aniline} = 2:1$ and the selectivity to AOB is 85.4%. With elevated temperature, the conversion of aniline is gradually increased and the selectivity to AOB is nearly unchanged (Table S2 in Supporting information). Aniline is quantitatively converted in 24 h at 70 °C, and the selectivity to AOB reaches up to 86.0%. No NSB is detected in the reaction (Table S2, entry 6). The results are indicative of quick transformation of the intermediate NSB. It is known that the products of the oxidation of aniline are light-sensitive. In order to understand the influence of natural light on the reaction results, the reaction in dark was carried out. Under optimized conditions, the reaction gives 92.0% aniline conversion and 88.8% selectivity to AOB (Table 1, entry 2). The conversion of aniline is slightly lower than that under natural light, and the products distribution is negligibly changed. Therefore, the following reactions were conducted under natural light.

Considering the weak compatibility of aniline in water, we also screened several organic solvents in which aniline is readily dissolved. The reactions in methanol (MeOH) and methyl *tert*–butyl ether (MTBE) give 61.7% and 65.3% conversion of aniline, respectively, much lower than that in water, despite of the slightly higher selectivity to AOB in MeOH (91.0%, Table S3 in Supporting information, entries 2 and 3). The reaction in mesitylene gives a conversion of 87.0%. However, the selectivity to AOB is only 52.6%, and the selectivity to NSB increases to 34.5% (Table S3, entry 4), suggesting the slow condensation of NSB with PHA in mesitylene. The oxidation of aniline was also carried out in neat acetic acid (HOAc). The conversion of aniline achieves to 100%. However, poor selectivity to each product is obtained (Table S3, entry 5). The reactions in *N*,*N*-dimethylformamide (DMF) and dimethyl sulfoxide (DMSO) give a low conversion of aniline (Table S3, entries 6 and 7). Unexpectedly, NSB becomes the dominant product in DMSO. The distinguishing product distribution in different solvents implies that these solvents may influence on different steps of the reaction. Water is regarded as the best solvent for present system. When the oxidant H_2O_2 is replaced by partially oil-soluble *tert*–butyl hydroperoxide (TBHP), only 6.1% aniline is converted under identical conditions, and NB becomes main by-product (31.8%, Table S4 in Supporting information, entry 1). The hydrophobicity of TBHP should be responsible for the result. Although *m*-chloroperbenzoic acid (*m*-CPBA) gives an aniline conversion of 94.1%, the selectivity to AOB is only 62.3% (Table S4, entry 2). These results reveal that H_2O_2 is the most suitable oxidant for present system. It is generally regarded that H_2O_2 is prone to decompose into O_2 under heating conditions. In order to check the effect of O_2 on the selective oxidation of aniline, some controlling experiments were carried out. The results show that the selective oxidation of aniline hardly proceeds in the absence of H_2O_2 under the ambiance of 1 atm air, O_2 and N_2, respectively, indicating that O_2 cannot affect the selective oxidation of aniline (Table S5 in Supporting information). We have tried to make a comparison of our present system with other reported systems in regard to the selective oxidation of aniline to AOB (Table S6 in Supporting information). The data imply that the catalytic activity of present system is attractive, especially when the use of water as the green solvent and the low ratio of $n_{H_2O_2}:n_{aniline}$ of present system are considered.

In order to further confirm the catalytic property of **1**, a series of controlling reactions were conducted. In the absence of catalyst, 59.4% aniline is converted in 24 h (Table 1, entry 3), much lower

Table 1
The selective oxidation of aniline with different catalyst.[a]

Entry	Catalyst	Conversion (%)	Selectivity (%)			
			NSB	NB	AB	AOB
1	**1**	99.4	0	6.7	7.3	86.0
2[b]	**1**	92.0	4.2	4.9	2.1	88.8
3	–	59.4	3.9	7.3	1.3	87.5
4	$Na_3PW_{12}O_{40}$	92.3	42.0	6.2	3.8	48.0
5[c]	$TBA_3PW_{12}O_{40}$	82.7	33.9	3.6	3.9	58.6
6[d]	**1**	85.4	1.7	8.2	2.5	87.6
7[e]	**1**	31.6	20.9	8.1	1.0	70.0
8[f]	**1**	25.1	25.9	8.4	2.0	63.7
9[g]	**1**	16.1	41.8	7.0	2.6	48.6
10	**2**	100	4.7	7.7	2.1	85.5
11	$Na_9PW_9O_{34}·nH_2O$	99.2	26.1	11.3	2.1	60.5
12[e]	$Na_9PW_9O_{34}·nH_2O$	94.1	33.0	10.9	2.3	53.8
13[f]	$Na_9PW_9O_{34}·nH_2O$	80.9	45.9	8.0	1.5	44.6
14[g]	$Na_9PW_9O_{34}·nH_2O$	78.3	66.9	6.2	0.9	26.0
15	$NiCl_2·6H_2O$	7.0	–	–	–	–
16	$Na_9PW_9O_{34}·nH_2O$+ $NiCl_2·6H_2O$	82.7	0	3.8	3.9	92.3

[a] Aniline 1 mmol, 30% H_2O_2 2 mmol, catalyst 0.75 mol% ($NiCl_2·6H_2O$ 4.5 mol%), 2 mL H_2O, 70 °C, 24 h.
[b] In dark.
[c] TBA = tetrabutylammonium.
[d] 12 h.
[e] 2 h.
[f] 1 h.
[g] 0.5 h.

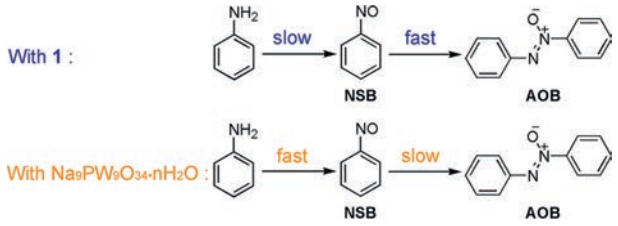

Scheme 2. The reaction patterns of the systems with **1** and $Na_9PW_9O_{34}\cdot nH_2O$.

than that with 0.75 mol% **1** (99.4%, Table 1, entry 1), suggesting the effectiveness of the catalyst. The performances of $Na_3PW_{12}O_{40}$ and $TBA_3PW_{12}O_{40}$ were also evaluated. The saturated polyanion $[PW_{12}O_{40}]$ gives good conversion of aniline, but the selectivity to AOB is much lower than that with **1** (Table 1, entries 4 and 5). When the reaction time with **1** is shortened to 12 h, 85.4% aniline is converted (Table 1, entry 6). However, the selectivity to AOB is nearly invariable, suggesting the condensation step is not the rate-determining step of the reaction. Further shortened reaction times such as 2 h, 1 h, and 0.5 h cause dramatic decrease of aniline conversion, but moderate to good selectivity to AOB are obtained (Table 1, entries 7–9). Compound **2** shows comparative performance with **1** (Table 1, entry 10). The precursor of **1** and **2**, $Na_9PW_9O_{34}\cdot nH_2O$, gives 99.2% conversion of aniline, but the selectivity to AOB is only 60.5%, while the amount of NSB dramatically increases to 26.1% (Table 1, entry 11), being indicative of the fast production of NSB or the suppression of the condensation step probably caused by the relative alkalinity of the trilacunary polyanion. We have also attempted to insight the reaction pattern with $Na_9PW_9O_{34}\cdot nH_2O$ by shortening the reaction time (Table 1, entries 12–14). Surprisingly, a relatively high aniline conversion of 78.3% is obtained in 0.5 h, and then slowly increases to 99.2% in 24 h. The selectivity to NSB decreases to 26.1% from 66.9%, and that to AOB contrarily increases to 60.5% from 26.0% with the prolonged reaction time. The results are apparently different from that with **1** as the catalyst. It is clear that in the reaction with $Na_9PW_9O_{34}\cdot nH_2O$, the condensation of NSB to AOB is the rate-determining step of the reaction. Apparently, the introduction of $\{Ni_6\}$ cluster into the skeleton of $Na_9PW_9O_{34}\cdot nH_2O$ successfully changes the catalytic behavior of $Na_9PW_9O_{34}\cdot nH_2O$ (Scheme 2). Besides, $NiCl_2\cdot 6H_2O$ shows negligible catalytic performance (Table 1, entry 15). When the mixture of $Na_9PW_9O_{34}\cdot nH_2O$ and $NiCl_2\cdot 6H_2O$ is used as the catalyst, 82.7% aniline is converted and the selectivity to AOB is 92.3% (Table 1, entry 16). The conversion is lower than that with pure $Na_9PW_9O_{34}\cdot nH_2O$. However, the selectivity to AOB with the mixture is much higher than that with pure $Na_9PW_9O_{34}\cdot nH_2O$ (60.5%), revealing that the presence of Ni^{2+} may slight depress the oxidation of aniline to NSB, but significantly promote the condensation of NSB to AOB. Prolonged reaction time and adjusted dosage of Ni^{2+} do not improve the conversion of aniline with the mixture (Table S7 in Supporting information). Based on these results, it is inferred that in the reactions with **1** and **2**, the elements W and Ni work cooperatively to guarantee the selective oxidation of aniline to AOB. The effect of $\{Ni_6\}$ on the reaction results can be explained from two aspects. On one hand, the $\{Ni_6\}$ cluster accelerates the condensation of NSB with PHA; on the other hand, the introduction of $\{Ni_6\}$ cluster may essentially change the electron structure of the matrix $\{PW_9\}$ and resultantly lead to the change of its redox property [38,39]. The point is also confirmed by the broadened UV–vis absorbance at 259 nm of compound **1**, which is ascribed to the $O_{2p}\rightarrow W_{5d}$ charge transfer, a common feature in all polyoxotungstates (Fig. S9 in Supporting information).

The substrate scope of the oxidative reaction system was also examined. Under optimized reaction conditions, methyl substituted

Table 2
1-Catalyzed selective oxidation of substituted anilines.[a]

Entry	Substrate	Conversion (%)	Product	Selectivity (%)
1		85.5	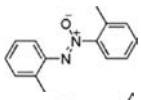	79.4
2		86.1	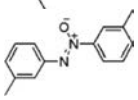	89.5
3		>99.9	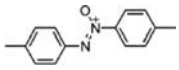	88.7
4		98.4	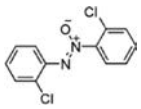	58.6
5		>99.9	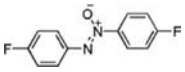	69.4
6		97.1	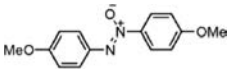	50.8
7[b]		72.1	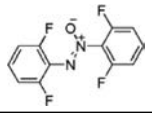	7.6

[a] Substrate 1 mmol, 30% H_2O_2 2 mmol, **1** 0.75 mol%, 2 mL H_2O, 70 °C, 24 h.
[b] Nitroso compound was detected as the main product (82.1%).

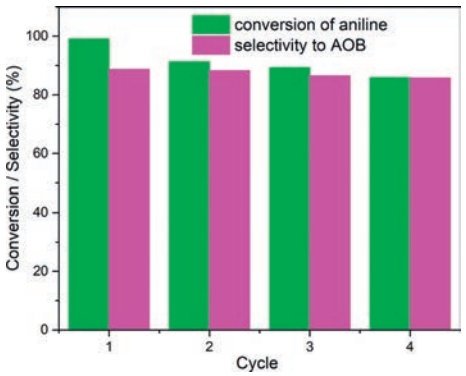

Fig. 2. The recyclability of aqueous phase including solid catalyst.

derivatives give excellent conversions and selectivities to corresponding azoxy compounds (Table 2, entries 1–3). Although 2-chloroaniline, 4-fluoroaniline, and 4-methoxyaniline are readily oxidized, moderate selectivities to azoxy compounds are obtained (Table 2, entries 4–6). The results reveal that the product distribution is sensitive to the reactivity of substrate itself. In case of 2,6-difluoroaniline, the conversion is 72.1% in 24 h (Table 2, entry 7). However, only trace azoxy compound is observed. Contrarily, nitroso compound becomes the main product (82.1%). It is deduced that the steric hindrance of difluoro significantly prevents the condensation of nitroso compound with hydroxylamine intermediate.

The stability of catalyst is always one of the most concerned topics. In this context, the stability of **1** was evaluated *via* spectroscopic and experimental tests. Initially, the catalyst was recovered after reaction by filtration. However, it is found that partial catalyst leaches into liquid phase. Thus, the recyclability of aqueous phase including solid catalyst was evaluated. After four reaction cycles, the conversion of aniline shows a minor decrease to 85.9% and the selectivity to AOB is nearly constant (Fig. 2). To elucidate the reason for the results, the solid catalyst was separated by centrifuga-

tion after complete removal of organic ingredients, and the activities of the recovered solid catalyst and the residual aqueous phase were respectively examined with accordingly reduced dosages of aniline, H_2O_2 and H_2O based on the hypothesis that no catalyst loss happen during the separation process of solid catalyst and aqueous phase. As a result, the conversion of aniline and the selectivity to AOB are 87.7% and 84.5%, respectively, when recovered solid catalyst is used (Table S8 in Supporting information). The results are indicative of the slight deactivation of the active sites for oxidative steps and can explain the minor decrease of aniline conversion in the cycling experiments. To check the structural integrity of the recovered catalyst, FT-IR, XPS and PXRD spectra of the sample before and after the catalytic process were compared. In the FT-IR spectra, two samples show nearly identical absorbance in the characteristic region for POM (600–1100 cm^{-1}) (Fig. S10a in Supporting information). The full XPS spectra confirm that all elements of pristine **1** are presented in the recovered solid catalyst (Fig. S10b in Supporting information), and the high-resolution spectra of the W 4f and Ni 2p show no visible difference between pristine **1** and recovered solid catalyst, suggesting that the exiting form and environment of them are unchanged (Figs. S11 and S12 in Supporting information). In the PXRD spectra, the positions of main peaks are unchanged after reaction but the relative intensities of them are changed owing to the lower crystallinity of **1** caused by the vigorous stirring during the reaction (Fig. S13 in Supporting information). All above information suggests that the structure of the recovered sample is retained well.

To understand the leaching species in the residual aqueous phase, the catalytic performance of the residual aqueous phase was initially checked. Resultantly, 93.2% aniline conversion and 86.7% AOB selectivity are respectively given, suggesting the structural integrity of the catalyst (Table S8). To confirm this point, the water in the aqueous phase was removed under reduced pressure at 40 °C. The obtained solid was also characterized by FT-IR, XPS and PXRD spectra. The FT-IR vibration, elemental composition and high-resolution XPS spectra of W 4f and Ni 2p are identical to those of the pristine **1** and the recovered solid catalyst (Figs. S10-S12). The PXRD spectrum of the obtained solid still shows the main peaks of **1**, despite the intensities of them are largely weakened (Fig. S13). These results indicate that the main species in the residual aqueous phase is integral **1**.

To gain insight into the reaction mechanism, 20 mol% 2,2,6,6-tetramethylpiperidine-1-oxyl several (TEMPO) has been added into the reaction system as the radical scavenger under the optimized conditions. Resultantly, the conversion of aniline decreases to 81.7% from 99.4% and the selectivity decreases to 72.0% from 86.0%, being indicative of the suppression of the reaction process. The results imply that the reaction involves some free radical intermediates, and TEMPO dramatically slows down the generation of PHA.

As is presented, 99.4% aniline is converted and the selectivity to AOB reaches up to 86.0% in 24 h under optimized conditions (Table 1, entry 1). When the reaction time is shortened to 4 h, only 50.4% aniline is converted and the selectivities to NSB, NB, AB, and AOB are 4.3%, 30.2%, 6.0% and 59.5%, respectively. In contrast, when 1 mmol PHA is used in place of aniline, it completely converts in 4 h, and the selectivity to AOB reaches up to 96.2%. Only trace NSB and NB are detected. The results suggest that the reaction rate of aniline is much slower than PHA. Thus, the initial step to PHA is the rate-determining step in the reaction of aniline.

According to the effectiveness of $Na_9PW_9O_{34}{\cdot}nH_2O$ and inertness of $NiCl_2{\cdot}6H_2O$ in the conversion of aniline (Table 1, entries 11–15), the active sites for oxidative steps are identified as W. The significant improvement of the selectivity to AOB in the reaction with the mixture of $Na_9PW_9O_{34}{\cdot}nH_2O$ and $NiCl_2{\cdot}6H_2O$ when compared to that with sole $Na_9PW_9O_{34}{\cdot}nH_2O$ implies that the $\{Ni_6\}$ cluster in **1** may contribute to the condensation of NSB with PHA.

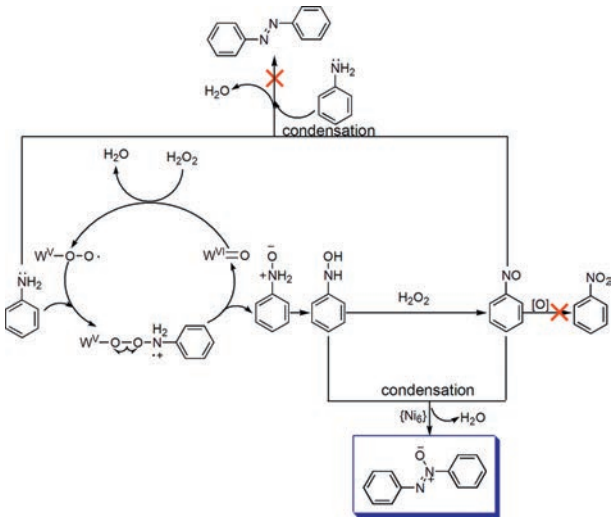

Scheme 3. Proposed mechanism.

To further confirm the point, the reaction of PHA in place of aniline was conducted. The reaction with $NiCl_2{\cdot}6H_2O$ as the catalyst gives high selectivity of 99.5% to AOB, and the conversion of PHA achieves to 99.4% in 1 h, while the reaction of PHA without catalyst gives 93.3% PHA conversion and 70.3% selectivity to AOB (Table S9 in Supporting information). The apparent difference of selectivity to AOB further confirms the function of Ni on the condensation of NSB with PHA. Besides, the rapid conversion of PHA in the absence of catalyst suggests that further oxidation of PHA may proceed readily without oxidative catalyst. In fact, the performances of $Na_3PW_{12}O_{40}$ and $TBA_3PW_{12}O_{40}$ also confirm the synergic effect of W and $\{Ni_6\}$ cluster (Table 1, entries 4 and 5). The good conversions for **1**, $Na_3PW_{12}O_{40}$ and $TBA_3PW_{12}O_{40}$ (99.4%, 92.3% and 82.7%, respectively) suggest that W is active for the oxidation step. However, the selectivities to AOB for them are quite different. The value for **1** is 86.0%, whereas those for $Na_3PW_{12}O_{40}$ and $TBA_3PW_{12}O_{40}$ are only 48.0% and 58.6%, respectively. Viewing from the structures of **1** and $[PW_{12}O_{40}]$, the $\{Ni_6\}$ cluster in **1** is in the place of $\{W_3\}$ cluster in $[PW_{12}O_{40}]$. The structure difference should be responsible for their selectivity difference, further confirming the effect of $\{Ni_6\}$ on the condensation step.

In order to further insight the reaction process, *in-situ* EPR test was performed with the expectation of finding the valence change of W and the information of involved radical. The spectrum shows a peak with g value of 1.9380 that can be ascribed to W^V ion generating in the reaction process [40,41]. The signal rises from unpaired paramagnetic electron at d orbit of W atom [42]. Synchronously, the signal with g value of 2.0031 suggests the presence of free radical (Fig. S14 in Supporting information).

Based on above results, a possible mechanism is proposed (Scheme 3). The catalytic process starts from the attack of $W^{VI}{=}O$ by H_2O_2 to generate tungsten peroxo radicals W^V-O-O·. The peroxo species are then quenched by aniline molecules to produce radical cationic intermediates in which the O–O bonds will undergo homolytic cleavage, leading to the recovery of $W^{VI}{=}O$ and the generation of PHA that subsequently undergoes further oxidation to generate NSB. In the following step, the condensation between PHA and NSB proceeds readily in the aid of the $\{Ni_6\}$ cluster. However, deep oxidation and condensation with aniline of NSB are prohibited.

In conclusion, two $\{Ni_6\}$ cluster involving POMs **1** and **2** were synthesized. The introduction of $\{Ni_6\}$ cluster into **1** and **2** efficiently modulates the catalytic property of $\{PW_9\}$ and leads to the selective oxidation of aniline to AOB that is attributed to the coop-

erative work of W and Ni sites in **1** and **2**. On one hand, the introduction of $\{Ni_6\}$ cluster changes the redox property of W site that is responsible for the oxidation steps of the reaction, and consequently impacts the rate of the oxidation step. On the other hand, the presence of $\{Ni_6\}$ cluster facilitates the condensation step of the reaction. The respective modulation of the oxidation and condensation steps results in the high selectivity to AOB of the intricate reaction. Therefore, the work provides an avenue to the development of bi-functional POM catalysts for highly selective multi-step reactions or one-pot cascade reactions.

Declaration of competing interest

The authors declare no conflict of interest.

Acknowledgments

This work was supported by the National Natural Science Foundation of China (Nos. 21773247, 22275185, 21521061, 21875252) and the Natural Science Foundation of Fujian Province (No. 2006L2005).

Supplementary materials

Supplementary material associated with this article can be found, in the online version, at doi:10.1016/j.cclet.2023.108324.

References

[1] Y.F. Liu, C.W. Hu, G.P. Yang, Chin. Chem. Lett. 34 (2023) 108097.
[2] S.S. Wang, G.Y. Yang, Chem. Rev. 115 (2015) 4893–4962.
[3] D. Vilona, M. Lelli, E. Dumont, E. Lacote, Chem. Eur. J. 27 (2021) 17761–17764.
[4] L.Y. Guo, S.Y. Zeng, Z. Jagličić, et al., Inorg. Chem. 55 (2016) 9006–9011.
[5] T.P. Hu, Y.Q. Zhao, Z. Jagličić, et al., Inorg. Chem. 54 (2015) 7415–7423.
[6] X. Huang, S. Liu, G. Liu, et al., Appl. Catal. B: Environ. 323 (2023) 122134.
[7] S.H. Talib, Z. Lu, X. Yu, et al., ACS Catal. 11 (2021) 8929–8941.
[8] Y. Wang, X.M. Chen, L.L. Zhang, C.G. Liu, Inorg. Chem. 28 (2019) 7852–7862.
[9] S.H. Talib, X. Yu, Q. Yu, S. Baskaran, J. Li, Sci. China Mater. 63 (2020) 1003–1014.
[10] L. Qiao, M. Song, A. Geng, S. Yao, Chin. Chem. Lett. 30 (2019) 1273–1276.
[11] Z. Zhang, Y. Li, E. Wang, et al., Inorg. Chem. 45 (2006) 4313–4315.
[12] Z. Wang, Q. Chen, Green Chem. 18 (2016) 5884–5889.
[13] Y. Benseghir, A. Lemarchand, M. Duguet, et al., J. Am. Chem. Soc. 142 (2020) 9428–9438.
[14] L. Jiao, Y. Dong, X. Xin, L. Qin, H. Lv, Appl. Catal. B: Environ. 291 (2021) 120091.
[15] H. Li, S. Yao, H.L. Wu, et al., Appl. Catal. B: Environ. 224 (2018) 46–52.
[16] Y. Zhao, Z. Wang, J. Gao, et al., Nanoscale 12 (2020) 21218–21224.
[17] X.X. Li, Y.X. Wang, R.H. Wang, et al., Angew. Chem. Int. Ed. 55 (2016) 6462–6466.
[18] J.S. Qin, D.Y. Du, W. Guan, et al., J. Am. Chem. Soc. 137 (2015) 7169–7177.
[19] Y.R. Wang, Q. Huang, C.T. He, et al., Nat. Commun. 9 (2018) 4466.
[20] J. Chen, W. Xu, M. Jiang, J. Chen, H. Jia, Appl. Catal. B: Environ. 278 (2020) 119263.
[21] T. Wang, M. Xu, X. Li, C. Wang, W. Chen, Inorg. Chem. Front. 7 (2020) 1676–1684.
[22] C. Chen, S. Mao, C. Tan, et al., Angew. Chem. Int. Ed. 60 (2021) 15556–15562.
[23] B. Yu, S. Zhang, X. Wang, Angew. Chem. Int. Ed. 60 (2021) 17404–17409.
[24] H. He, G. Wang, S. Chai, et al., Chin. Chem. Lett. 32 (2021) 2013–2016.
[25] S. He, Q. Liu, X. Wang, J. Mater. Chem. A 10 (2022) 5758–5770.
[26] X.B. Han, Z.M. Zhang, T. Zhang, et al., J. Am. Chem. Soc. 136 (2014) 5359–5366.
[27] S.S. Zhang, J.Y. Chen, K. Li, et al., Chem. Mater. 33 (2021) 9708–9714.
[28] X.B. Han, C. Qin, X.L. Wang, et al., Appl. Catal. B: Environ. 211 (2017) 349–356.
[29] H. Lv, W. Guo, K. Wu, et al., J. Am. Chem. Soc. 136 (2014) 14015–14018.
[30] L. Yu, Y. Ding, M. Zheng, H. Chen, J. Zhao, Chem. Commun. 52 (2016) 14494–14497.
[31] A. López-Benítez, A. Guevara-Lara, G. Berhault, ACS Catal. 9 (2019) 6711–6727.
[32] S. Han, Y. Cheng, S. Liu, et al., Angew. Chem. Int. Ed. 60 (2021) 6382–6385.
[33] W. Chen, H. Li, Y. Jin, et al., Chem. Commun. 58 (2022) 9902–9905.
[34] H. Li, M. Yang, Z. Yuan, et al., Chin. Chem. Lett. 33 (2022) 4664–4668.
[35] J. Qin, Y. Long, F. Sun, et al., Angew. Chem. Int. Ed. 61 (2022) e202112907.
[36] J. Goura, B.S. Bassil, X. Ma, et al., Chem. Eur. J. 27 (2021) 15080–15084.
[37] S.S. Wang, X.Y. Kong, W. Wu, et al., Inorg. Chem. Front. 9 (2022) 4350–4358.
[38] E.N. Glass, J. Fielden, Z. Huang, et al., Inorg. Chem. 55 (2016) 4308–4319.
[39] E.N. Glass, J. Fielden, A.L. Kaledin, et al., Chem. Eur. J. 20 (2014) 4297–4307.
[40] J.Z. Liao, H.L. Zhang, S.S. Wang, et al., Inorg. Chem. 54 (2015) 4345–4350.
[41] R. Prados, M.T. Pope, Inorg. Chem. 15 (1976) 2547–2553.
[42] X. Chen, Y. Lin, J. Sol-Gel Sci. Technol. 36 (2005) 197–201.